STRUCTURAL ANALYSIS OF THE KSC-28 STORABLE TRANSPORT CASK

J.H. Ku, K.S. Seo, D.K. Min and S.G. Ro
Korea Atomic Energy Research Institute, Korea
Korea

Y.J. Kim
Sungkyunkwan University, Korea

ABSTRACT

The KSC-28 cask has been developed for storage and transportation of spent fuels by KAERI Korea. This paper describes the structural evaluation of KSC-28 cask for impact accidents. Since this cask contains large amount of spent fuels, the structural analysis of the large cask considered carefully the complex internal structure and the influence of spent fuels' inertia effect. The structural analyses were carried out using LS-DYNA3D code for various impact conditions. The impact forces, stresses, and deformations were evaluated for each impact condition. The results demonstrate that the KSC-28 cask maintains its structural integrity sufficiently for impact accidents.

INTRODUCTION

The KSC-28 cask has been developed for storage and transportation of spent fuels by Korea Atomic Energy Research Institute (KAERI) in Korea. The dual purpose cask must meet all the design requirements for transportation as well as storage. As specified in domestic regulations and the IAEA standards (IAEA 1990), this cask must maintain its structural integrity during the normal transport and the hypothetical accident conditions. The load conditions should be chosen for causing the maximum damage of the cask. KSC-28 cask can transport and store 28 PWR spent fuel assemblies with a 10 years of cooling time. Since this cask contains large amount of spent fuels weighing about 18 tons, the structural analysis of the large cask should consider carefully the complex internal structure and the influence of spent fuels' inertia effect. The impact analyses were carried out for KSC-28 cask by finite element analysis using LS-DYNA3D code (LSTC 1995). This paper describes the dynamic impact behaviors of the cask for various impact conditions.

ANALYSIS

The KSC-28 cask consists of a cask body and impact limiters. The cask body consists of stainless steel shells and forgings for the structural members, lead for the gamma shield and silicone mixture for the neutron shield. The multi-layered structural shells consist of inner shell, intermediate shell, and outer shell. The impact limiters are constructed from stainless steel casings and wood blocks. The steel casing has internal gussets which enclose the wood blocks. Balsa wood and redwood are used for shock absorbing materials. The outer diameter of the cask body is 2.5 m, the body length is 4.8 m, and the total loaded weight of cask is about 110 tons.

The structural analysis of KSC-28 cask was carried out by three dimensional analysis models using LS-DYNA3D code. A half-section of the cask was modeled using symmetric geometry and the symmetry boundary condition was applied to all nodes located at symmetry plane. Fig. 1 shows the structural analysis

models used for the impact analysis. Fig. 1(a) shows 9-m horizontal drop model consisted of 40,472 nodes, 24,096 solid elements and 8,279 shell

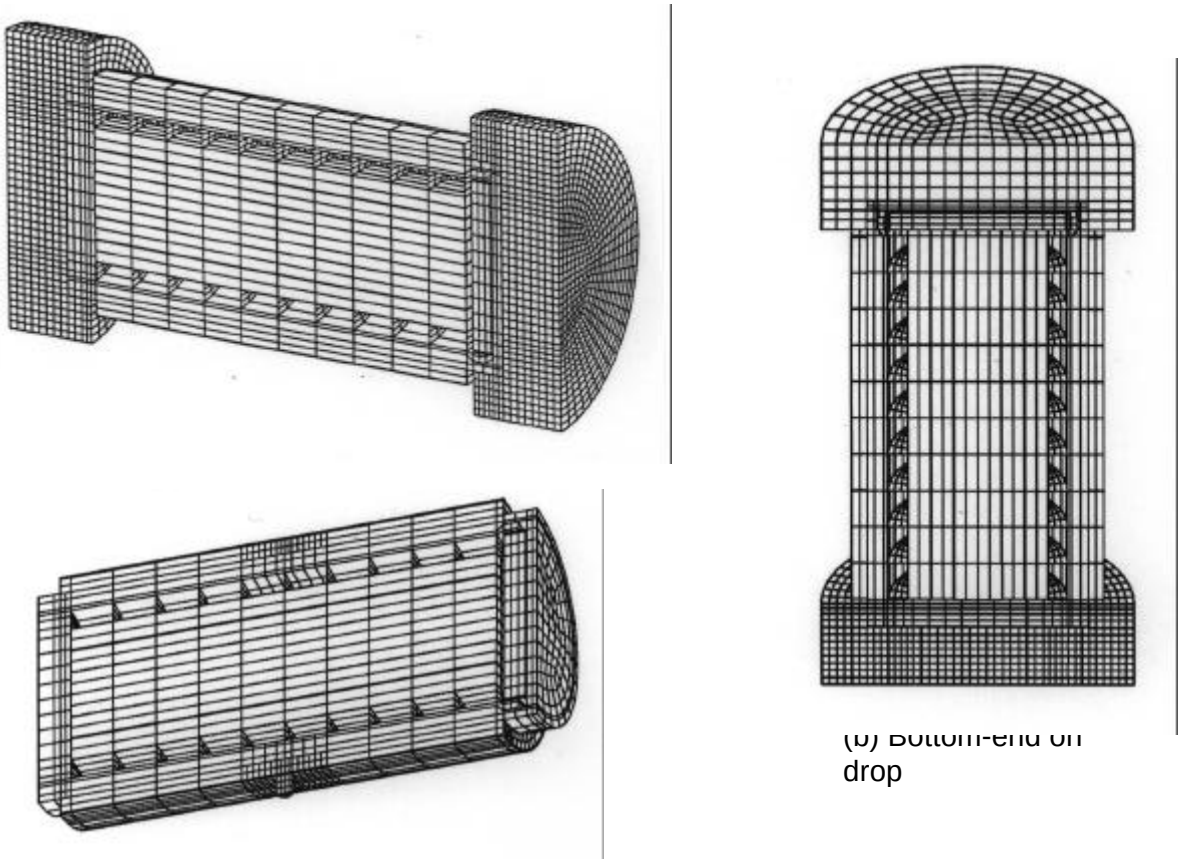

Fig. 1 Impact analysis models of KSC-28 cask.

elements. For the bottom-end on drop analysis, the top impact limiter parts were replaced by coarse mesh. For puncture analysis, the impact limiters were removed for direct impact of the cask onto a steel bar without interference of impact limiters.

The analysis model consists of several components such as structural members, shields, impact limiters and internal structures as well as dummy fuels. Since the interfaces between the stainless steel structures and shielding materials are remained in simple contact state instead of chemical bonding, several parts of the components were modeled separately and assembled together. These interfaces between the materials were considered using automatic contact elements. The interfaces of the bolted area between the cask body and impact limiters were constrained by combining their retaining parts with tied interfaces. For simplicity, the bolted area of the cask lid was constrained to the cask body by rigid nodal constraint condition.

The metal structure of steel case and gusset plates were modeled by shell elements. The interfaces between the steel case and wood blocks and the grain direction arrangements were taken into account, because the balsa wood and the redwood blocks are inserted into the steel case in axial and radial directions, and they have orthogonal crush characteristics (Attaway and Yoshimura 1989, Cramer et al. 1995). Fuel baskets and basket retaining plates were modeled using shell elements, and spent fuel assemblies were modeled using solid elements with an equivalent density, according to the load combination regulations, as described

in Regulatory Guide 7.8 (U.S. NRC 1989). For the impact analysis of the empty cask, these fuel elements were omitted. All analysis results were compared with the results of the empty cask.

All material properties were assumed as elastic-plastic with strain hardening modulus for the exact simulation as possible. Though the Regulatory Guide 7.6 (U.S. NRC 1978) requires the elastic analysis for containment boundaries, the concern of this study is focused on the exact impact behavior. The late tendency for structural analysis is establishing non-linear dynamic analysis criterion of the cask for more accurate characterization of the cask response under accident loading.

The initial velocity of 13.3 m/sec was applied to all nodes as a load condition in a direction normal to the stonewall. This impact velocity is consistent with a free drop height of 9m. Other loads, such as internal pressure, were neglected, because there were not the concern of this study. The unyielding target was simulated by stone wall option as an infinite flat rigid surface fixed in the space, and all nodes which were expected to be contacted with the target surface were modeled as sliding with void interface element.

ANALYSIS RESULTS

Figure 2 shows a comparison of the impact force-time histories of empty and fuel loaded casks acting on the target for 9-m bottom-end on drop. This figure shows that the analysis results of the 9-m bottom-end on drop were very similar, except for a small difference in magnitude. The maximum impact forces were 72 MN at 17 ms after impact initiation for the empty cask, and 81 MN at 18 ms for the loaded cask. The impact behaviors were very similar with each other, but impact force was increased about 12% and impact duration was increased 3 ms for the loaded cask. Figure 3 shows the deformed shapes and stress contours of the loaded KSC-28 cask. The maximum deformations of the impact limiter were 147 mm for the loaded cask and 143 mm for the empty cask at 22 ms.

The maximum stresses of the loaded cask were 75 MPa in inner shell and 87 MPa in intermediate shell at 16 ms. For the empty cask, the maximum stresses were 80 MPa and 84 MPa each, and there were no significant difference. However, for the bottom part, which receives the impact force of spent fuels directly, the maximum stress was increased by about 39%, from 74 MPa to 103 MPa.

Figure 4 shows a comparison of the impact force-time histories of empty and fuel loaded casks acting on the target for 9-m horizontal drop. This figure shows a larger difference in magnitude than for the bottom-end on drop. The maximum impact force of the loaded cask was 72 MN at 37 ms, and the impact force was decreased rapidly after 38 ms. The maximum deformation of the impact limiter for the loaded cask was 306 mm at 37 ms, and this time was much delayed compared to the bottom-end on drop. However, the maximum impact force of the empty cask was decreased significantly by about 42%, to 50 MN at 27.5 ms. Fig. 5 shows the comparison of stress time-histories for 9m horizontal drop.

The impact duration of the empty cask for horizontal drop impact was much shortened than for bottom-end on drop. The maximum deformation of the impact limiter was decreased by about 19% as 254 mm at 33 ms. Fig. 6(a) and (b) show the deformed shapes and stress contours of loaded cask for horizontal drop impact. The maximum stresses in the shells were 81 MPa at inner shell and 93 MPa at intermediate shell at 30 ms after impact. The maximum stresses in the shells of empty cask were decreased by up to 20% compared to loaded cask as 65 MPa at inner shell and 82 MPa at intermediate shell.

Fig. 7 shows deformed shape and stress contour of KSC-28 cask under puncture impact. The maximum stresses were 225 MPa in the intermediate shell and 227 MPa in the inner shell.

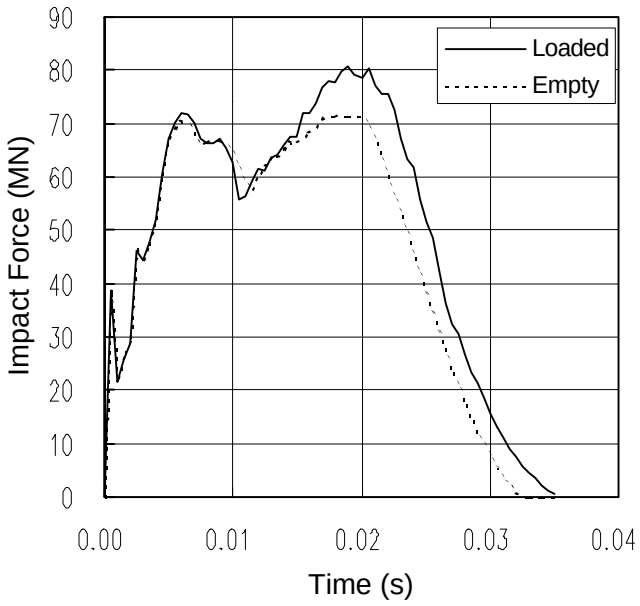

Fig. 2 Comparison of impact force-time histories for a 9m bottom-end drop.

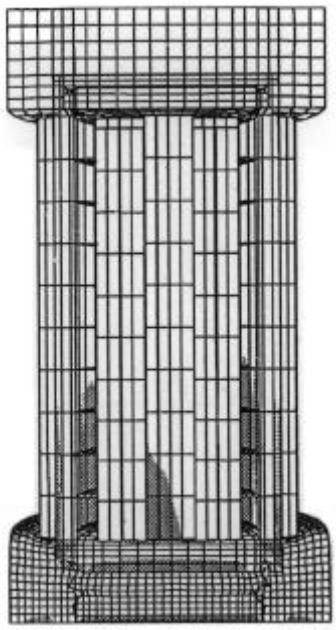

Fig. 3 Deformed shape and stress contour of KSC-28 cask under a 9m bottom-end on drop

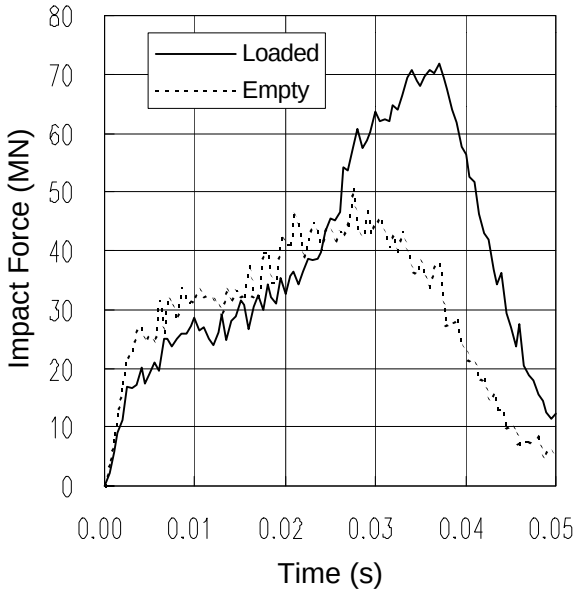

Fig. 4 Comparison of impact-time histories for a 9m horizontal drop.

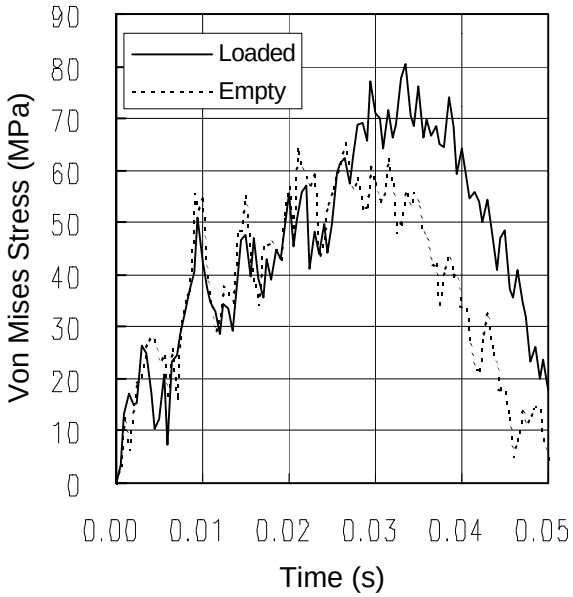

Fig. 5 Comparison of stress-time histories for a 9m horizontal drop.

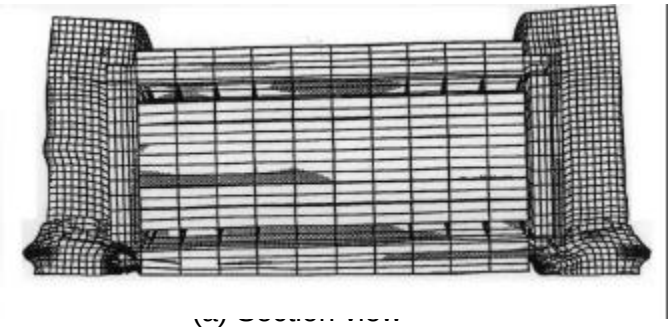

(a) Section view

(b) Outside view

Fig. 6 Deformed shape and stress contour of the KSC-28 cask under a 9m horizontal drop.

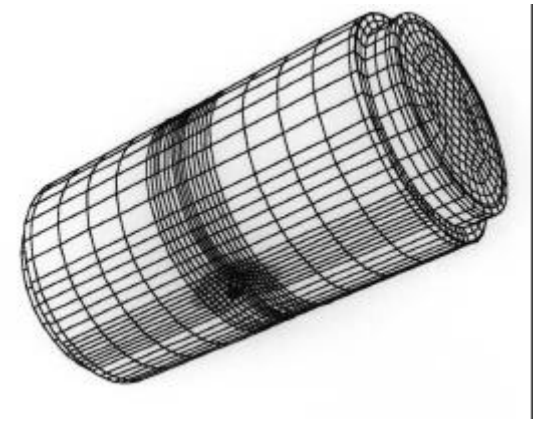

Fig. 7 Deformed shape and stress contour of the KSC-28 cask under puncture impact.

DISCUSSION

For the vertical drop impact, the impact force of the loaded cask was increased by about 12% compared to the empty cask. The impact behaviors were very similar to each other, and the stresses in shells were not much affected by the loaded fuels in the cask. However, the bottom structural part, which receives the inertia load of the fuels directly, was much affected. On the contrary, for the horizontal drop impact, the weights of the loaded fuels directly affected the bottom part of the shells. This means that the increased inertia force due to the fuel weight of 18 tons (about 16% of total cask weight), so affects the parts related directly to the impact that the stresses in these parts are increased so significantly.

For vertical drop impact, the impact force is increased suddenly with the initiation of impact, gradually increased as the deformation rate of the impact limiter is decreased, and then decreased rapidly as the cask rebounds. For the vertical drop impact, the entire bottom area of the impact limiter is contacted with the target surface simultaneously, whereas, for horizontal drop, the flank of the cylindrically shaped impact limiter is contacted in the normal direction to the tangent.

Contrary to vertical drop impact, horizontal drop impacts showed different results for empty and loaded casks, as shown in Fig. 4. For horizontal drop impact of the empty cask, the maximum deformation of the impact limiter was 254 mm, and most of the impact energy was absorbed by this deformation. For loaded cask, the maximum deformation of the impact limiter was 313 mm. If the deformation of the impact limiter

exceeds 292 mm, the outer shell and neutron shield layer are deformed together with the impact limiters. Therefore, the secondary rapid increase of the impact force time history started at the contact initiation of outer shell with the target surface.

In horizontal drop impact, the maximum stresses of the shells were higher than the stresses in the vertical drop impact, despite the larger deformations of impact limiters and longer impact duration. There are two reasons for these high stresses. Firstly, the total volume of the impact limiters participating in energy absorption is insufficient. The impact limiters absorb initial impact force very well because the cross sectional area related to energy absorption starts with a small area and then increases as impact is advanced. However, the total volume of the impact limiters which related to impact is small, and so some portion of the cask outer shell is impacted on the target plane, as shown in Fig. 6(b). Therefore, the peak impact force is increased, in spite of the small initial impact force and impact retardation effect. Secondly, the cask is impacted in the flank so that most of the loads act on one side of cylindrical shells.

For puncture impact, the outer shell and neutron shield is deformed very much and the maximum stress of the outer shell exceeded the yield stress. However it was limited to the local area near to the impacted part and the inner shell maintained its structural integrity without damage.

CONCLUSIONS

From the inspection of the analysis results, it was concluded that the KSC-28 cask maintains its structural integrity under the impact accidents. The spent fuels loaded in the cask increased the impact force than the empty cask in impact accidents by their inertia. The internal stress of the structural part and deformation of impact limiters are also increased by the inertia load of the fuels. Most of the impact force in vertical drop is absorbed by the deformation of the impact limiter for both loaded cask and empty cask. However, in horizontal drop, some portion of the impact force is absorbed by the deformation of the outer shell and the neutron shield besides the impact limiters when the fuels are loaded. Therefore, horizontal drop is more affected by the inertia load of loaded fuels than vertical drop. The impact energy absorption by the deformation of the outer shell and the neutron shield in horizontal seems inevitable, therefore should be considered together with the deformation of the impact limiters.

The inertia load of load fuels are an important factor which should be considered in impact analysis. They especially have an important effect on the stress of structural parts near the point of impact, and therefore may change the stress distributions of the cask.

REFERENCES

Attaway S.W. and Yoshimura H.R., "Dynamic and Static Behavior of Metal Gussets in Cask Impact Limiters", *The 9th International Symposium on the Packaging and Transportation of Radioactive Materials*, **1**, *p55*, 1989.

Attaway S.W. and Yoshimura H.R., "A Local Isotropic/Global Orthotropic Finite Element Technique for Modeling the Crush of Wood in Impact Limiters", *The 9th International Symposium on the Packaging and Transportation of Radioactive Materials*, **1**, *p63*, 1989.

Cramer et al., "Crush Performance of Redwood for Developing Design Procedures for Impact Limiters", *Proceedings of the 11th International Conference on the Packaging and Transportation of Radioactive Materials*, p875, 1995.

Hallquist J.O. et al., "LS-DYNA3D User's Manual (Nonlinear Dynamic Analysis of Structures in Three Dimensions)", *LSTC Report 1007 Rev. 3*, Livermore Software Technology Corp., 1995.

"Regulations for the Safe Transport of Radioactive Material", 1985 Edition as amended in 1990, *IAEA Safety Series No. 6*, 1990.

"Load Combinations for the Structural Analysis of Shipping Casks for Radioactive Material", *Regulatory Guide 7.8*, U.S. Nuclear Regulatory Commission, Rev.1, 1989.

"Design Criteria for the Structural Analysis of Shipping Cask Containment Vessels", *Regulatory Guide 7.6*, U.S. Nuclear Regulatory Commission, Rev.1, 1978.